DOI 10.1002/mnfr.201400539 *Mol. Nutr. Food Res.* 2015, *59*, 520–532

RESEARCH ARTICLE

High-fat diet induces endothelial dysfunction through a down-regulation of the endothelial AMPK–PI3K–Akt–eNOS pathway

Concha F. García-Prieto[1], Francisco Hernández-Nuño[1], Danila Del Rio[1], Gema Ruiz-Hurtado[2,3], Isabel Aránguez[2,4], Mariano Ruiz-Gayo[1], Beatriz Somoza[1] and María S. Fernández-Alfonso[2]

[1] Departamento de Ciencias Farmacéuticas y de la Salud, Facultad de Farmacia, Universidad CEU-San Pablo, Madrid, Spain
[2] Instituto Pluridisciplinar and Departamento de Farmacología, Facultad de Farmacia, Universidad Complutense, Madrid, Spain
[3] Unidad de Hipertensión, imas12, Hospital 12 de Octubre, Madrid, Spain
[4] Departamento de Bioquímica, Facultad de Farmacia, Universidad Complutense, Madrid, Spain

Received: August 4, 2014
Revised: November 8, 2014
Accepted: November 13, 2014

Scope: Activation of endothelial adenosine monophosphate-activated protein kinase (AMPK) contributes to increase nitric oxide (NO) availability. The aim of this study was to assess if high-fat diet (HFD)-induced endothelial dysfunction is linked to AMPK deregulation.
Methods and results: Twelve-week-old Sprague Dawley male rats were assigned either to control (10 kcal % from fat) or to HFD (45 kcal % from fat) for 8 wk. HFD rats segregated in obesity-prone (OP) or obesity-resistant (OR) rats according to body weight. HFD triggered an impaired glucose management together with impaired endothelium-dependent relaxation, reduced endothelial AMPK activity and lower NO availability in aortic rings of OP and OR cohorts. Relaxation evoked by AMPK activator, 5-aminoimidazole-4-carboxamide-1-β-d-ribofuranoside (AICAR) was reduced in both OP and OR rings, which exhibited lower p-AMPKα-Thr^{172}/AMPKα ratios that negatively correlated with plasma non-esterified fatty acids (NEFA) and triglycerides (TG). Inhibition of PI3K (wortmannin, 10^{-7} M) or Akt (triciribine, 10^{-5} M) reduced relaxation to AICAR only in the control group ($p < 0.001$). Akt (p-Akt-Ser^{473}) and eNOS phosphorylation (p-eNOS-Ser^{1177}) were significantly reduced in OP and OR ($p < 0.01$).
Conclusion: Endothelial dysfunction caused by HFD is related to a dysfunctional endothelial AMPK–PI3K–Akt–eNOS pathway correlating with the increase of plasma NEFA, TG, and an impaired glucose management.

Keywords:
Adenosine monophosphate-activated protein kinase / Endothelial function / High-fat diet / Obesity-prone / Obesity-resistant

Additional supporting information may be found in the online version of this article at the publisher's web-site

1 Introduction

The AMP-activated protein kinase (AMPK) is a ubiquitously distributed Ser/Thr kinase. It is a sensor of cellular energy status that is activated to restore energy balance after depletion

Correspondence: Dr. María S. Fernández-Alfonso, Instituto Pluridisciplinar, Paseo Juan XXIII, 1. 28040, Madrid, Spain
E-mail: marisolf@farm.ucm.es
Fax: +34-913943264

Abbreviations: **+E**, with endothelium; **–E**, endothelium free; **ACh**, acetylcholine; **AICAR**, 5-aminoimidazole-4-carboxamide-1-β-d-ribofuranoside; **AMPK**, adenosine monophosphate-activated protein kinase; **ANOVA**, analysis of variance; **AUC**, area under the concentration-response curves; **BW**, body weight; **CaMKKβ**, calcium/calmodulin-dependent protein kinase kinase-β; **DIO**, diet-induced obesity; **EMax**, maximum response; **eNOS**, endothelial nitric oxide synthase; **GTT**, intraperitoneal glucose tolerance test; **HFD**, high-fat diet; **LKB1**, liver kinase B1; **NEFA**, non-esterified fatty acids; **NO**, nitric oxide; **OLETF**, Otsuka Long Evans Tokushima Fatty; **OP**, obesity-prone; **OR**, obesity-resistant; **Phe**, phenylephrine; **SD**, Sprague Dawley; **SNP**, sodium nitroprusside; **SOD**, superoxide dismutase; **TG**, triglycerides

of energy stores [1, 2]. AMPK is the downstream component of a protein kinase cascade that is activated by the rise in cellular AMP:ATP ratio and thus switches off ATP-consuming anabolic pathways via phosphorylation or regulation of enzymes relevant for energy storage [1, 2].

AMPK is expressed in the vasculature in both endothelial [3] and smooth muscle cells [4]. In cultured endothelial cells, activation of AMPK has been shown to stimulate endothelial nitric oxide synthase (eNOS) phosphorylation at Ser^{1177} and Ser^{633} and NO availability [5, 6] through the Akt–eNOS [7] and/or PI3K–Akt–eNOS [8] pathways. Whole vessel studies suggest that AMPK modulates vascular function through endothelium-dependent and independent mechanisms. In conduit arteries, AMPK increases eNOS phosphorylation at Ser^{1177} [9] and enhances endothelium-dependent vasodilatation [10,11], although the pathway linking both events has not been characterized yet. Similar findings have been observed in resistance vessels of the rat [12] and humans [13]. AMPK also regulates myosin-light chain kinase activity by decreasing the sensitivity of vascular smooth muscle to intracellular Ca^{++}, thus reducing vascular tone [14]. Direct pharmacological activation of vascular AMPK by metformin [15] or 5-aminoimidazole-4-carboxamide-1-β-d-ribofuranoside, AICAR [15,16] as well as by hypoxia [17] leads to a decrease in cholesterol synthesis [18] and to an increase in fatty acid oxidation [19,20]. All these data strongly suggest a protective role of AMPK on vascular function. Accordingly, genetic models of metabolic syndrome, such as Zucker diabetic fatty and Otsuka Long Evans Tokushima Fatty (OLETF) rats, exhibit endothelial dysfunction associated to AMPK dysregulation [21, 22].

The substantial interest in the AMPK cascade as a possible therapeutic target for the treatment of vascular complications in metabolic disorders warrants the characterization of the pathway, linking AMPK activation to NO release and endothelial relaxation in whole vessels ex vivo. Moreover, there are no studies assessing the impact of diet-induced obesity (DIO), which better resembles human obesity, on endothelial AMPK activity and vascular function. The hypothesis of this study is that obesity induced by energy dense diets leads to a reduced AMPK activity contributing to a diminished NO availability and endothelial dysfunction. The aim of this study is to first characterize ex vivo the signaling pathway involved in AMPK-induced NO increase, as well as the contribution of endothelial AMPK to relaxation in whole aortas ex vivo. Second, we analyze if a high-fat diet (HFD) leads to alterations in endothelial AMPK–NO pathway that might correlate with a reduced endothelial function.

2 Materials and methods

2.1 Animals and dietary treatments

Twelve-week-old Sprague Dawley (SD) male rats (Harlan, Barcelona, Spain; 250–300 g) were housed under controlled dark-light cycles (12h/12h from 8:00 am to 8:00 pm) and temperature (22°C) with standard food and water ad libitum. After 1 wk, animals were housed individually, divided into two groups with a similar mean body weight (BW), and assigned either to a control diet (D12450B, 10% of energy from fat, 70% from carbohydrates, and 20% from protein; 3.78 kcal/g; $n = 10$) or to a high-fat diet (HFD, D12451, 45% of energy from fat, 35% from carbohydrates, and 20% from protein; 4.65 kcal/g; $n = 20$) (Test Diet Limited BCM IPS Ltd., London, UK). After 4 wk of diet, HFD rats were subdivided in obesity-prone (OP) and obesity-resistant (OR) animals according to BW on the basis of BW increase. HFD rats exhibiting BW increase in the range of the control group BW (50.32 ± 4.78 g) were assigned to the obesity-resistant group ($n = 10$, OR). HFD rats over these limits were considered as obesity-prone individuals ($n = 10$; OP). Animals had free access to food during 4 additional weeks, during which BW and food intake were monitored twice a week. On day 49^{th} of dietary treatment, rats were fasted from 8 am until 2 pm for intraperitoneal glucose tolerance test. The last day, rats were weighed and killed by decapitation at 9 am. Blood was collected in chilled EDTA-coated polypropylene tubes. To minimize alterations in AMPK activity or phosphorylation, 24-h fasting was omitted to avoid lipolysis and any eventual reduction of mesenteric perivascular adipose tissue amount [23]. Biochemical values represent therefore postprandial concentrations. Plasma samples were frozen for biochemical determinations. Adipose tissues were weighed and normalized by tibia length. Thoracic aortas were used for both vascular function and western blot studies. The investigation conforms to the *Guide for the Care and Use of Laboratory Animals* published by the US National Institute of Health (NIH publication No. 85-23, revised in 2011) and was approved by the Ethics Committee of Universidad CEU-San Pablo (BFU2011-25303).

2.2 Plasma measurements

Insulin was determined by using of a specific EIA kit (Mercodia, Uppsala, Sweden; 1.8% intra-assay variation and 3.8% inter-assay variation) for rat insulin. Glucose was measured by a spectrophotometric method (Glucose Trinder Method, Roche, Barcelona, Spain). Triglycerides (TG) and non-esterified fatty acids (NEFA) were determined using GPO (Biolabo, Maizy, France) and ACS-ACOD (Wako, Germany) methods, respectively.

2.3 Intraperitoneal glucose tolerance test (GTT)

During the last week of dietary treatment, rats were fasted during 6 h before glucose load (i.p. bolus of 1 g/kg at time 0). Blood glucose level was measured immediately at 0, 15, 30, 60, and 120 min after injection. At the indicated times, blood samples were drawn from tail vein of conscious rats

for glucose determination with Accu-Check Aviva glucometer (Roche Diagnostics, Mannheim, Germany).

2.4 Vascular reactivity in the thoracic aorta artery

Vascular reactivity was performed in an organ bath setting as previously described [24]. Briefly, aortic rings of 2 mm length were given an optimal resting tension of 1.5 g, which was readjusted every 15 min during a 60-min equilibration period. Isometric tension was recorded in a Power Lab system (ADInstruments, Oxford, UK). Before starting the experiment, rings were contracted with 75 mM KCl to assess their contractility. Endothelial integrity was analyzed by addition of acetylcholine (ACh, 10^{-9} to 10^{-4} M) and endothelium-independent response was evaluated in presence of sodium nitroprusside (SNP, 10^{-10} to 10^{-5} M) to segments pre-contracted with phenylephrine (Phe, 10^{-7} M). Segments with more than 60% relaxation to 10^{-4} M ACh were considered with endothelium (+E) and segments with less than 10% relaxation to 10^{-4} M ACh were considered as endothelium-free (–E). N_G-nitro-L-arginine methyl ester (L-NAME, 10^{-4} M) and indomethacin ($3{\cdot}10^{-6}$ M) were preincubated for 20 min.

Protocol 1: Basal vascular AMPK activity was estimated by comparing the relaxation to ACh (10^{-9} to 10^{-4} M) in absence/presence of Compound C (10^{-5} M, 25 min), an AMPK inhibitor, in aortic rings +E.

Protocol 2: In another set of experiments, +E and –E aortic rings were pre-contracted with Phe (10^{-7} M), and then treated with AICAR (10^{-5} to $8{\cdot}10^{-3}$ M), an AMPK activator. This nucleoside is taken up by the cell and accumulates in the cytoplasm as the monophosphorylated derivative, 5′-aminoimidazole-4-carboxamide-ribonucleoside, an AMP analogue that activates AMPK without disturbing cellular adenine nucleotide ratio [25]. In some experiments, the PI3K inhibitor wortmannin (10^{-7} M), the Akt inhibitor triciribine (10^{-5} M), or the nitric oxide synthases (NOS) inhibitor L-NAME (10^{-4} M) were added into the bath 25 min before Phe administration.

2.5 Western blot analysis

Aortas from control, OP, and OR rats were isolated in PSS solution [24] and cleaned of blood and perivascular fat. In some segments, endothelium was removed by gentle rubbing. Western blotting was performed as previously described [26]. Briefly, 30–40 μg protein samples were separated by SDS-PAGE gels. Primary antibodies anti-phospho-liver kinase B1 [p-LKB1 (Ser^{428})] and LKB1 (1:1000 final dilution; Cell Signaling Technology, Massachusetts, USA), calcium/calmodulin-dependent protein kinase kinase-β (CaMKKβ, 1:1000 final dilution; Santa Cruz Biotechnology, Germany), p-AMPKα (Thr^{172}) and AMPKα (1:1000 final dilution; Cell Signaling Technology), PI3Kα-110 (1:800 final dilution; Cell Signaling Technology), p-PI3K p85 (Tyr^{458}) and PI3K p85 (1:1000 final dilution; Cell Signaling Technology), p-Akt (Ser^{473}) and Akt (1:1000 final dilution; Cell Signaling Technology), p-eNOS (Ser^{1177}) (1:800 final dilution; Cell Signaling Technology), eNOS (1:800 final dilution; BD Transduction Laboratories, Lexington, UK), iNOS (1:5000 final dilution; BD-Transduction Laboratories), Mn-superoxide dismutase (Mn-SOD) and Cu/Zn-SOD (1:1000 final dilution; Santa Cruz Biotechnology), extracellular SOD (EC-SOD, 1:1000 final dilution; Enzo Life Sciences, USA), $p47^{phox}$ and $p22^{phox}$ (1:500 final dilution; Santa Cruz Biotechnology) and catalase (1:2000 final dilution, Sigma-Aldrich, Spain) were applied overnight at 4°C. After washing, appropriate secondary antibodies (anti-rabbit or anti-mouse IgG-peroxidase conjugated) were applied for 1 h at a dilution of 1:5000. Blots were washed, incubated in commercial enhanced chemiluminescence reagents (ECL Prime, Amersham Bioscence, UK) and bands were detected by ChemiDoc XRS+ Imaging System (Bio-Rad, California, USA). To prove equal loadings of samples, blots were re-incubated with β-actin antibody (1:5000 final dilution; Sigma-Aldrich, Missouri, USA). Blots were quantified using Image Lab 3.0 software (Bio-Rad, USA). Values for p-LKB1, p-AMPKα, p-PI3K p85, p-Akt, and p-eNOS were normalized with LKB1, AMPKα, PI3K p85, Akt, and eNOS, respectively.

2.6 Data analyses

All values are given as mean ± SEM and n denotes the number of animals used in each experiment. Statistical significance was analyzed by using either one-way or two-way analysis of variance (ANOVA) followed by Bonferroni or Newman–Keuls post hoc test for comparison between groups. A value of $p < 0.05$ was considered statistically significant. KCl responses are expressed as absolute values. In vascular reactivity experiments, contractions are expressed as the percentage of contraction produced by 75 mM KCl. Relaxations are expressed as the percentage of a previous Phe contraction. The maximum response (EMax values) was calculated by nonlinear regression analyses of each individual concentration-response curve. Area under the concentration-response curves (AUC) were calculated from the individual concentration-response curve plots (GraphPad Software, California, USA).

2.7 Chemicals

ACh was dissolved in saline and Phe and SNP in 0.01% ascorbic acid/saline (Sigma-Aldrich, USA). Indomethacin was prepared in ethanol and both L-NAME (Sigma-Aldrich, USA) and AICAR (Toronto Research Chemicals, Canada) in water. Compound C, wortmannin, and triciribine were dissolved in DMSO and were provided by Sigma-Aldrich (USA).

Table 1. Effect of HFD on tissue weights and plasma parameters

	Control	OP	OR
Lumbar adipose tissue (g/cm)	0.53 ± 0.07	0.90 ± 0.05***	0.66 ± 0.05$^{\#\#}$
Mesenteric adipose tissue (g/cm)	0.85 ± 0.08	1.23 ± 0.08**	0.91 ± 0.04$^{\#\#}$
Subcutaneous adipose tissue (g/cm)	0.45 ± 0.05	0.63 ± 0.05*	0.49 ± 0.04$^{\#}$
Liver (g/cm)	2.97 ± 0.12	2.95 ± 0.10	2.91 ± 0.05
Plasma glucose (mg/dL)	96.70 ± 5.31	98.29 ± 4.90	100.9 ± 8.41
Plasma TG (mg/dL)	54.38 ± 12.32	165.4 ± 30.61**	119.4 ± 13.81*
Plasma NEFA (mg/dL)	9.83 ± 1.39	19.14 ± 2.14**	16.24 ± 1.10**
Plasma insulin (ng/mL)	2.75 ± 0.69	3.44 ± 0.58	2.12 ± 0.34

Tissue weights are expressed in g per cm tibia length, which was not different between groups.
$^{*}p < 0.05$, $^{**}p < 0.01$, and $^{***}p < 0.001$ versus control group;
$^{\#}p < 0.05$ and $^{\#\#}p < 0.01$ versus OP group (one-way ANOVA, Newman–Keuls post hoc test). Data are expressed as mean ± SEM ($n = 7$–9).

3 Results

3.1 Body weight, adiposity, and plasma parameters

After 8 wk of HFD, BW was similar between OR and control rats, whereas it was significantly increased in OP rats (Supporting Information Fig. 1A). As shown in Table 1, HFD significantly increased lumbar, mesenteric and subcutaneous adipose tissue weight in the OP, but not in the OR group. These changes were not attributable to differences in food intake since this was similar between groups (Supporting Information Fig. 1B). Plasma NEFA and TG were significantly higher in both OP and OR groups compared to control animals (Table 1). No differences were observed in glucose or insulin levels. However, GTT shows a worse management of glucose in OP and OR than in control rats (Supporting Information Fig. 2) ($AUC_{control} = 15171 \pm 341.5$; $AUC_{OP} = 18954 \pm 799$, $p < 0.001$; $AUC_{OR} = 18042 \pm 515.8$, $p < 0.01$).

3.2 Endothelial function is reduced in both OP and OR groups due to a lower NO availability

In intact arteries, ACh (10^{-9} to 10^{-4} M) elicited a concentration-dependent relaxation which was significantly reduced in both OP and OR animals compared to the control group (Fig. 1A). We detected a negative correlation between EMax of ACh and plasma NEFA, plasma TG or AUC of GTT in all control, OP and OR animals (Supporting Information Fig. 3). In contrast, endothelium-independent relaxation elicited by SNP (10^{-10} to 10^{-5} M, Fig. 1B) as well as contraction to 75 mM KCl (control = 1.91 ± 0.06 g; OP = 2.12 ± 0.10 g; OR = 1.98 ± 0.08 g) were similar in all experimental groups, excluding alterations in contractile machinery of the media.

The relative contribution of endothelial factors involved in ACh-evoked relaxation was then analyzed separately (Fig. 1C). Pre-incubation with indomethacin ($3{\cdot}10^{-6}$ M) had no significant effect on ACh-induced relaxation in none of the three groups (Fig. 1C), excluding prostanoids contribution. However, endothelial relaxation to ACh was completely abolished by L-NAME (10^{-4} M) in controls, but was only partially reduced in both OP and OR groups (Fig. 1C). The difference between AUC in presence or absence of L-NAME, which indirectly indicates basal NO release, was significantly lower after HFD independently of the group ($AUC_{control} = 275.12 \pm 3.21$; $AUC_{OP} = 175.25 \pm 23.13$, $p < 0.01$; $AUC_{OR} = 165.35 \pm 9.52$, $p < 0.001$), suggesting a reduction in NO availability. Concentration-response relaxation to ACh in presence of L-NAME (10^{-4} M) plus indomethacin ($3{\cdot}10^{-6}$ M) (Supporting Information Fig. 4) was completely abolished in control, but only partially reduced in both OP and OR groups. This result suggests the contribution of other vasodilatory mechanisms (probably of a hyperpolarizing factor) to compensate reduced NO bioavailability in response to HFD.

3.3 Basal AMPK was reduced in both OP and OR groups

In order to explore whether the reduction in NO availability was linked to AMPK activity, we characterized relaxation to ACh (10^{-9} to 10^{-4} M) in presence of the inhibitor of AMPK, Compound C (10^{-5} M). We observed that response to ACh was significantly reduced in all three groups (Fig. 2A). Quantitative AUC analysis in presence or absence of Compound C, which indirectly reflects basal AMPK activity, revealed that difference in AUC was significantly lower in both OP and OR than in the control group (Fig. 2B).

3.4 HFD induces endothelial but not muscular AMPK down-regulation

Relaxation to the AMPK activator, AICAR, was characterized in both +E and –E arteries in order to evaluate the partial contribution of endothelial and muscular AMPK. In +E segments, relaxation to AICAR (10^{-5} to $8{\cdot}10^{-3}$ M) was significantly higher in control arteries ($EMax_{control} = 76.49 \pm 3.65\%$)

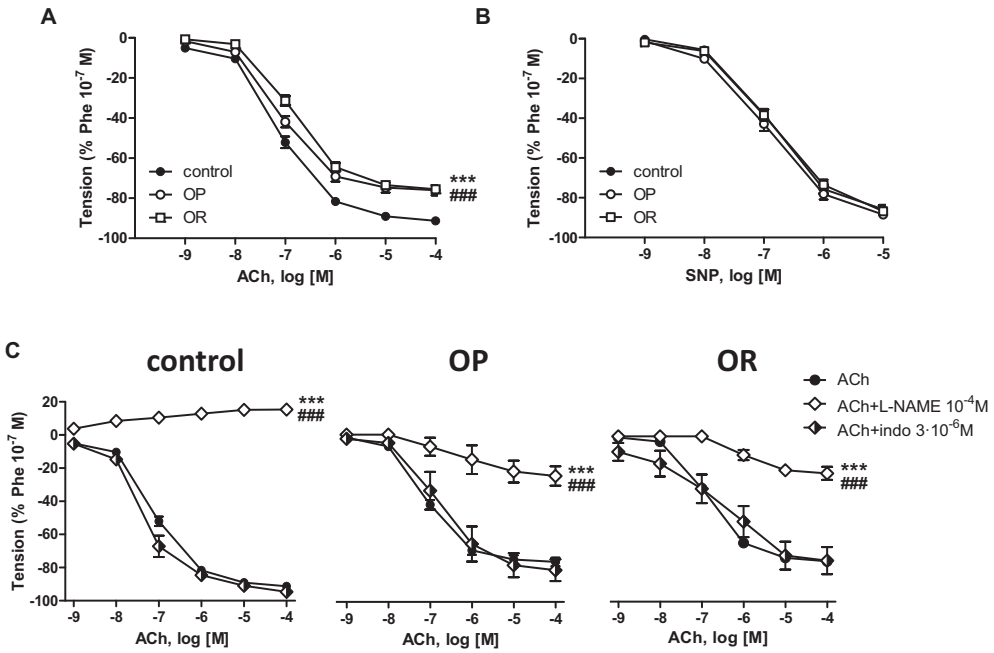

Figure 1. (A) Cumulative concentration-response curves to ACh (10^{-9} to 10^{-4} M). $^{***}p < 0.001$ OP versus control group; $^{\#\#\#}p < 0.001$ OR versus control group (two-way ANOVA, Bonferroni post hoc test; $n \geq 7$). (B) Endothelium-independent relaxation to SNP (10^{-9} to 10^{-4} M) ($n \geq 5$). (C) Cumulative concentration-response curves to ACh with or without L-NAME (10^{-4} M) and indomethacin (indo, $3{\cdot}10^{-6}$ M). $^{***}p < 0.001$ compared to their corresponding matched ACh curves; $^{\#\#\#}p < 0.001$ compared to their corresponding indomethacin treatment (two-way ANOVA, Bonferroni post hoc test; $n \geq 4$). All data are means ± SEM.

compared with the OP ($EMax_{OP} = 57.47 \pm 4.22\%$) or the OR ($EMax_{OR} = 50.25 \pm 5.17\%$; $p < 0.01$) groups (Fig. 3A). Endothelial removal significantly reduced AICAR-induced relaxation in the control group, suggesting a significant contribution of endothelial AMPK to AICAR-induced relaxation. In both OP and OR animals, however, no differences were observed in AICAR-induced relaxation between intact and endothelium-denuded segments, suggesting that HFD selectively altered endothelial AMPK.

To further confirm this result, p-AMPKα (Thr^{172})/AMPKα ratios were quantified in +E (Fig. 3B) and –E arteries (Fig. 3C). We observed a significant reduction of p-AMPKα (Thr^{172})/AMPK-α in intact arteries from OP and OR animals compared to controls (Fig. 3B), whereas no difference was

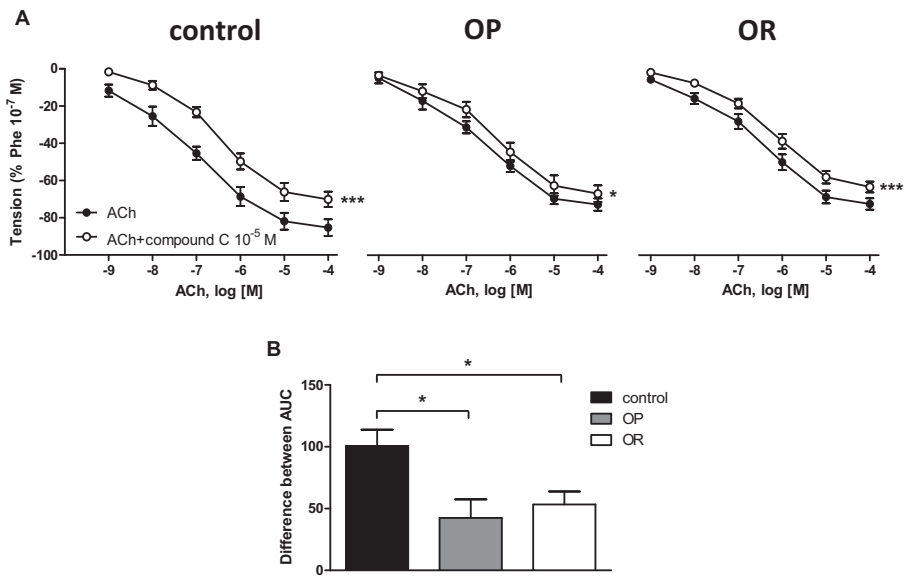

Figure 2. (A) Cumulative concentration-response curves to ACh (10^{-9} to 10^{-4} M) in absence/presence of AMPK inhibitor, compound C (10^{-5} M). $^{*}p < 0.05$ and $^{***}p < 0.001$ compared to their corresponding matched ACh curves (two-way ANOVA, Bonferroni post hoc test; $n \geq 5$). (B) Differences between areas under concentration-response curves to ACh in presence/absence of Compound C. $^{*}p < 0.05$ compared to control animals (one-way ANOVA, Newman–Keuls post hoc test; $n \geq 5$). All data are means ± SEM.

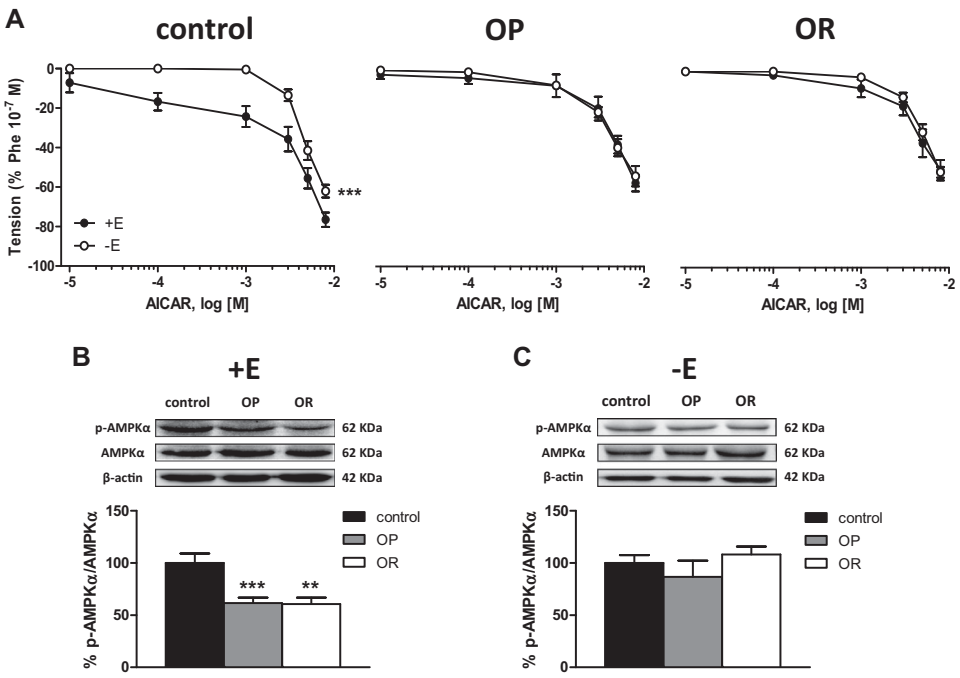

Figure 3. (A) Cumulative concentration-response curves to AMPK activator (AICAR, 10^{-5} to $8{\cdot}10^{-3}$ M) in aorta with (+E) and without (–E) endothelium. $^{***}p < 0.001$ compared to their corresponding matched +E curves (two-way ANOVA, Bonferroni post hoc test; $n \geq 5$). Data are means ± SEM. (B, C) Representative immunoblots of p-AMPKα (Thr^{172}) in +E (B) and −E aortas (C) and densitometric analysis expressed as percentage of p-AMPKα (Thr^{172})/AMPKα in the control group ± SEM. $^{**}p < 0.01$ and $^{***}p < 0.001$ compared to control animals (one-way ANOVA, Newman–Keuls post hoc test; $n \geq 5$).

observed in –E arteries between groups (Fig. 3C). A negative correlation was found between p-AMPKα (Thr^{172})/AMPKα and plasma NEFA or TG levels in intact aorta from control, OP and OR animals (Supporting Information Fig. 5A and 5B).

3.5 HFD induces a down-regulation of AMPK-kinases, LKB1, and CaMKKβ

To determine the molecular mechanism leading to p-AMPKα down-regulation, protein levels of upstream AMPK-kinases were determined. Both LKB1 and p-LKB1 (Ser^{428}) expression was significantly reduced in OP and OR compared to control rings (Fig. 4A). A similar result was observed for CaMKKβ (Fig. 4B).

3.6 HFD induces a down-regulation of endothelial PI3K–Akt–eNOS pathway

To characterize the pathway connecting endothelial AMPK to NO production, we designed a set of experiments in +E arteries in which AICAR-induced relaxation was sequentially analyzed with inhibitors of PI3K (wortmannin), Akt (triciribine) and eNOS (L-NAME). Moreover, the goal of these experiments was to establish whether endothelial AMPK–PI3K–Akt–eNOS pathway is altered in DIO.

Wortmannin (10^{-7} M) significantly reduced relaxation to AICAR (10^{-5} to $8{\cdot}10^{-3}$ M) in the control but not in the OP nor OR groups (Fig. 5A). Western blot analysis revealed that PI3Kα-110 (a catalytic subunit of PI3K) was significantly reduced only in the OR group (Fig. 5B), whereas neither p-PI3K p85 (Tyr^{458}) nor PI3K p85 (a regulatory subunit of PI3K) were different between groups (Fig. 5C).

Relaxation to AICAR (10^{-5} to $8{\cdot}10^{-3}$ M) in presence of triciribine (10^{-5} M) was reduced in the control but not in the OP nor OR groups (Fig. 6A). A significant reduction of p-Akt (Ser^{473})/Akt was observed in intact arteries from OP and OR animals compared to control (Fig. 6B). We detected a negative correlation between p-Akt (Ser^{473})/Akt and AUC of GTT in all control, OP and OR animals (Supporting Information Fig. 5C).

L-NAME (10^{-4} M) significantly reduced relaxation to AICAR (10^{-5} to $8{\cdot}10^{-3}$ M) in control and OP aortic segments, but not in the OR group (Fig. 7A). Relaxation and difference in AUC between curves in presence and absence of L-NAME were significantly lower between control and OP or OR group, respectively (Fig. 7B). These results indicated a lower NO release in HFD animals. In both OP and OR groups, p-eNOS (Ser^{1177})/eNOS level was significantly reduced compared to the control group (Fig. 7C). To further analyze the effect of L-NAME in the OP group, a possible induction of iNOS was assessed. The expression of iNOS was significantly higher in the OP compared to both control and OR groups (Fig. 7D), suggesting an up-regulation of iNOS only in OP animals.

3.7 HFD induces a down-regulation of mitochondrial SOD

The expression of the mitochondrial SOD isoform, Mn-SOD, was significantly reduced in both OP and OR rings (Fig. 8A). However, no differences between groups were observed for

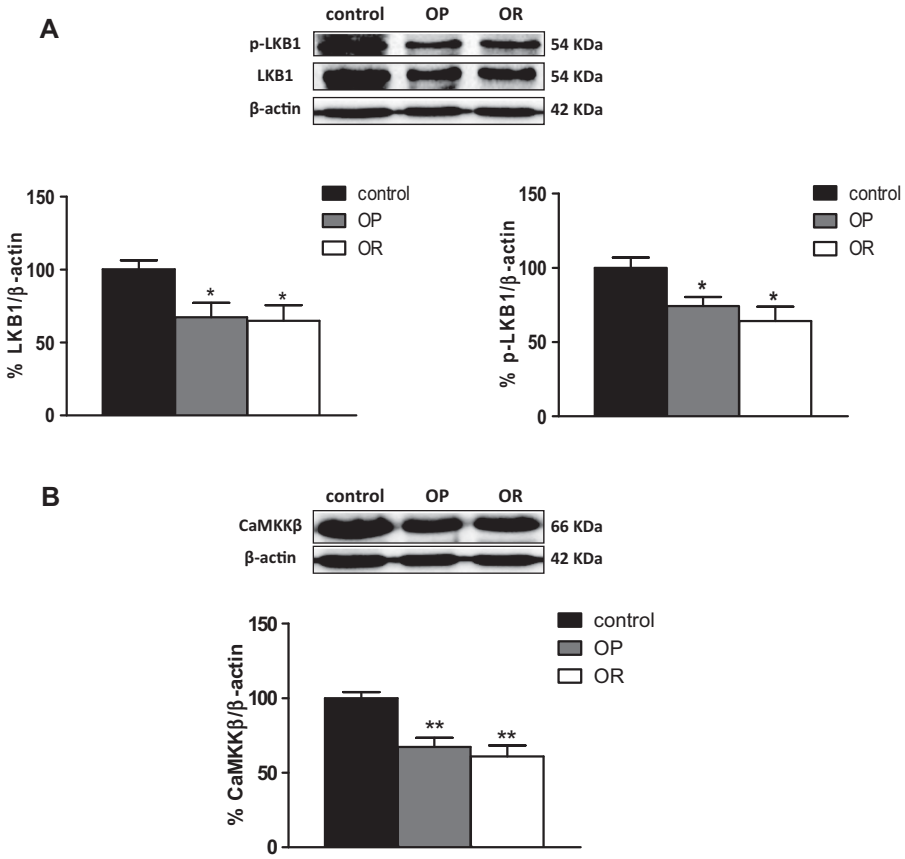

Figure 4. Western blot analysis of upstream AMPK-kinases LKB1 and CaMKKβ. (A) Representative immunoblots of LKB1 and p-LKB1 (Ser^{428}) in +E aorta and densitometric analysis expressed as percentage of LKB1/β-actin and p-LKB1(Ser^{428})/β-actin, respectively, in the control group ± SEM. $*p < 0.05$ compared to the control group (one-way ANOVA, Newman–Keuls post hoc test; $n = 5$). (B) Representative immunoblots of CaMKKβ in +E aorta and densitometric analysis expressed as percentage of CaMKKβ/β-actin in the control group ± SEM. $**p < 0.01$ compared to the control group (one-way ANOVA, Newman–Keuls post hoc test; $n = 5$).

the cytosolic Cu/Zn-SOD and extracellular SOD (EC-SOD) (Fig. 8B and C).

To determine if elevated superoxide levels could contribute to reduce NO bioavailability, expression of the NADPH oxidase subunits, $p47^{phox}$ and $p22^{phox}$, was assessed. No differences were observed between groups for both $p47^{phox}$ (control = 100 ± 13.72%, OP = 99.86 ± 12.94% and OR = 86.39 ± 19.94%) and $p22^{phox}$ (control = 100 ± 12.46%, OP = 99.88 ± 29.97% and OR = 113.10 ± 14.40%). These results suggest that the reduction in NO bioavailability is not due to NADPH oxidase activation.

Protein levels of catalase, another important antioxidant, were similar between groups (control = 100 ± 4.99%, OP = 88.49 ± 3.49% and OR = 101.30 ± 29.08%).

4 Discussion

The present study shows for the first time that AMPK-induced NO increase is mediated by activation of the PI3K–Akt–eNOS pathway in whole vessels ex vivo. HFD specifically impairs endothelial AMPK-mediated relaxation through the down-regulation of this pathway, as well as AMPK-kinases LKB1 and CaMKKβ. This down-regulation is independent of BW gain and correlates with NEFA and TG levels, as well as with GTT profiles in both OP and OR rats. We propose that HFD-induced endothelial impairment is associated to a down-regulation of the AMPK–PI3K–Akt–eNOS pathway in endothelial cells probably related to high lipid levels and impaired glucose management.

Here we first show that AICAR-induced relaxation in aorta of control SD rats is mediated by stimulation of both endothelial and muscular AMPK. Relaxation to AICAR is more efficient in intact aortic rings and it seems exclusively mediated by NO, suggesting a prominent contribution for the endothelial AMPK–NO pathway to vascular relaxation. Our results are in agreement with previous studies showing that AMPK modulates vascular function in conduit arteries through both endothelium-dependent and independent mechanisms [9–11], although an endothelium-derived contractile factor has been also suggested to be involved in AICAR response [10].

This study also demonstrates that the endothelial AMPK–PI3K–Akt–eNOS pathway accounts for an adequate endothelial function in whole aorta. Although previous studies show that AMPK activation increases NO availability through eNOS phosphorylation at Ser^{1177} [5,6,9], the cascade downstream of AMPK had not been properly identified in whole vessels. To rule out a potential nonspecific activity of compound C [27] or AICAR [28], functional results were confirmed by determining protein expression of p-AMPKα (Thr^{172}), PI3K-α110, p-Akt (Ser^{473}) and p-eNOS (Ser^{1177}) ex vivo. Our results are in

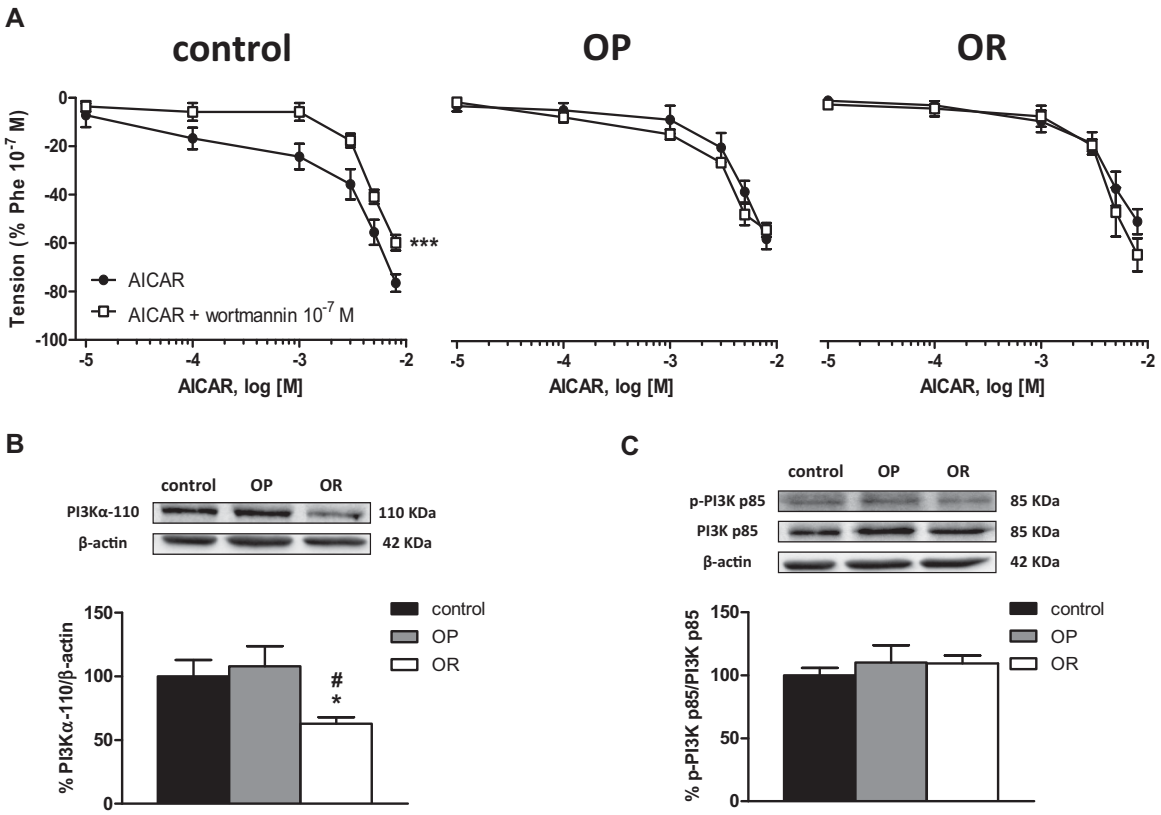

Figure 5. (A) Cumulative concentration-response curves to AICAR (10^{-5} to $8{\cdot}10^{-3}$ M) in aorta +E in presence/absence of PI3K inhibitor (wortmannin, 10^{-7} M). ***$p < 0.001$ compared to their corresponding matched AICAR curves (two-way ANOVA, Bonferroni post hoc test; $n \geq 4$). Data are means ± SEM. (B) Representative immunoblot of catalytic subunit of PI3K (PI3Kα-110) in +E aorta and densitometric analysis expressed as percentage of PI3Kα-110/β-actin in the control group ± SEM. *$p < 0.05$ compared to control group; #$p < 0.05$ compared to OP group (one-way ANOVA, Newman–Keuls post hoc test; $n = 6$). (C) Representative immunoblot of regulatory subunit of PI3K (PI3K p85) in +E aorta and densitometric analysis expressed as percentage of p-PI3K p85 (Tyr^{458})/PI3K p85 in the control group ± SEM ($n = 6$).

accordance to previous studies in cultured endothelial cells showing that AMPK activation stimulates eNOS phosphorylation [5, 6] through Akt [7] or PI3K–Akt [8].

Since AMPK functions as a fuel sensor that is activated by energy depletion, it is conceivable to hypothesize that HFD-induced obesity leads to AMPK down-regulation. Here we show that DIO selectively alters endothelial-dependent relaxation to AICAR in both OP and OR groups, due to a decrease of endothelial p-AMPKα (Thr[172]) levels that leads to a desensitization of PI3Kα-110, p-Akt (Ser[473]), p-eNOS (Ser[1177]), and ultimately to the impairment of endothelial function. PI3Kα-110 plays an important role by regulating cell proliferation and survival in heart [29] and endothelial cells [30]. Although an eventual decrease in PI3Kα-110 expression in OP animals under long-term HFD cannot be excluded, our current data only show a down-regulation of this protein in the OR group. This finding suggest that OR animals might show an increase in endothelial cells apoptosis and vascular hypertrophy, that could contribute to relaxation impairment in this group. The molecular mechanism leading to lower p-AMPKα levels seems to involve a decrease in the activity of the AMPK-kinases, LKB1 and CaMKKβ. Although we have not determined ATP levels, it might be speculated that ATP would be increased in an environment of energy surplus. In this context, Thors et al. [31] have demonstrated in cultured endothelial cells that AMPK is activated by both LKB1 and CaMKK under conditions of low ATP, and by CaMKK alone when intracellular ATP remains unchanged [31].

Although dysregulation of vascular AMPK has been observed in genetic models of metabolic syndrome, such as Zucker diabetic fatty [21] and OLETF rats [22], this is the first study demonstrating endothelial AMPK dysfunction in response to HFD and suggesting that surplus energy input leads to endothelial damage through the down-regulation of the AMPK–PI3K–Akt–eNOS cascade.

The precise role played by AMPK in endothelial cell metabolism remains poorly understood. AMPK phosphorylates acetyl-CoA-carboxylase and thereby increases fatty acid oxidation [19, 20]. Moreover, it is becoming clear that endothelial AMPK plays a central role in regulating both mitochondrial function and biogenesis, thus playing a pivotal role in oxidative stress [32]. Several studies have shown that

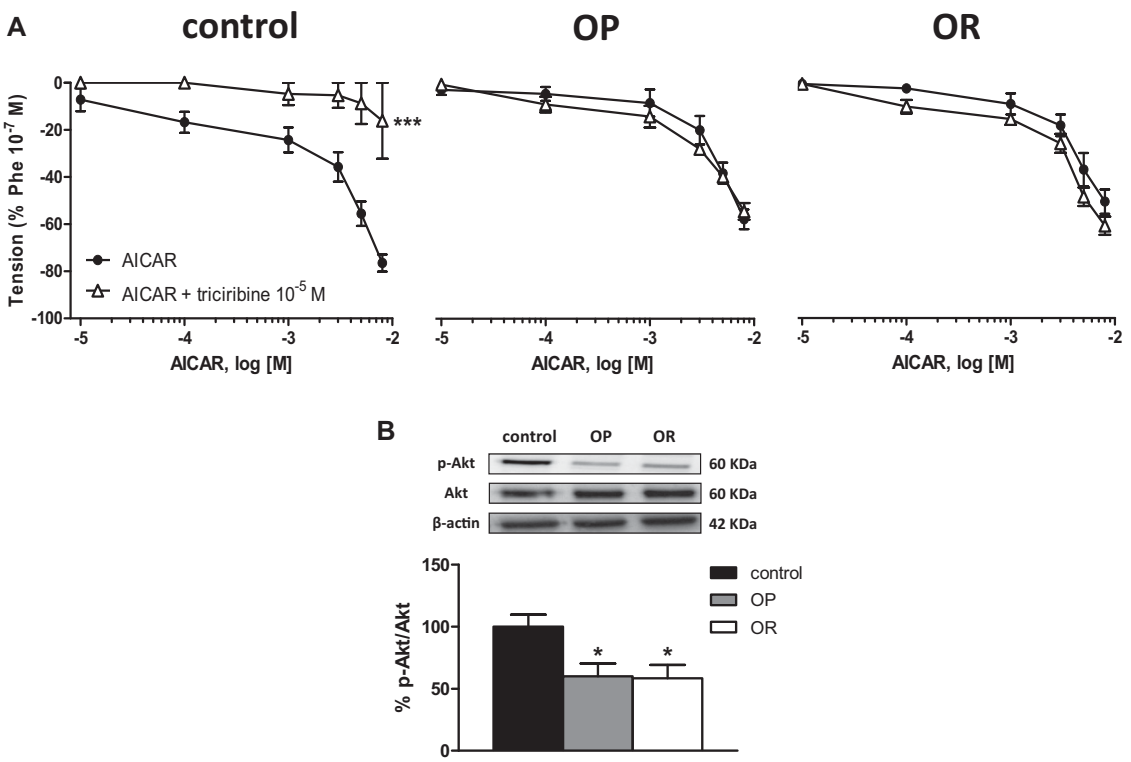

Figure 6. (A) Cumulative concentration-response curves to AICAR (10^{-5} to $8{\cdot}10^{-3}$ M) in presence/absence of Akt inhibitor (triciribine, 10^{-5} M) in +E aorta. ***$p < 0.001$ compared to their corresponding matched AICAR curves (two-way ANOVA, Bonferroni post hoc test; $n \geq 4$). Data are means ± SEM. (B) Representative immunoblots of p-Akt (Ser^{473}) in +E aorta and densitometric analysis expressed as percentage of p-Akt (Ser^{473})/Akt in the control group ± SEM. *$p < 0.05$ compared to the control group (one-way ANOVA, Newman–Keuls post hoc test; $n = 6$).

increased fatty acids availability reduces the activity of AMPK in heart and liver of rodents [33, 34]. At the vascular level, the decrease in AMPK activity in endothelial cells of obese OLETF rats parallels lipid accumulation, apoptosis and a reduction of NO, which are associated with the impairment of endothelial-dependent relaxation [22]. Inhibition of AMPK has been also observed in C57BL/6J mice fed a palmitate-enriched HFD [35]. Moreover, long-term high levels of fatty acids trigger ceramide-protein phosphatase 2A-dependent inhibition of both AMPK and eNOS [35]. Bakker et al. [36] proposed that increased availability of TG and long chain fatty acyl-CoA in endothelial cells could cause oxidative stress by affecting the mitochondrial respiratory chain. The dramatic reduction in Mn-SOD, which is the only known scavenger of superoxide anion in the mitochondrial matrix, suggests that superoxide levels would be increased locally in the mitochondria, thus contributing to mitochondrial dysfunction. Although Mn-SOD is not the most expressed SOD isoform at the vascular wall, it plays a critical role as first line of defense in protecting the mitochondria from superoxide anion produced as by-product of the respiratory chain [37, 38]. In fact, reduced Mn-SOD activity in vivo correlates to both increased oxidative damage and alteration in mitochondrial function [39]. Our current results suggest that mitochondrial damage triggered by HFD would contribute to endothelial injury and dysfunction in fatty acid enriched environments.

In the present study, we used a modification of the rat DIO model originally developed by Levin et al. [40]. This model enables to dissociate between factors related to HFD from obesity per se. SD rats fed a moderately HFD exhibit a bimodal pattern of BW gain similar to that observed in humans. Half of the rats gain weight rapidly compared with chow-fed rats (OP), whereas the other half gain weight at a similar rate to that of the chow-fed animals (OR). Using this model, several studies demonstrated that OP, but not OR rats, exhibit cardiometabolic complications, such as hypertension, hypercholesterolemia, hyperinsulinemia, renin-angiotensin system activation and increased renal oxidative stress [41–44]. Here we observe, however, that endothelial function is reduced in OP as well as in OR groups probably due to the higher amount of fat in our diet (45% of calories from fat) compared to the original model fed with a diet containing 32% kcal from fat. In fact, the impairment of endothelium-dependent relaxation (EMax), as well as the reduction in p-AMPKα (Thr^{172}) expression, negatively correlates with the increase in NEFA and TG levels, which are similar in both OP and OR groups. In this context, we suggest that the similarities between OP and OR are related to the HFD and rich fatty acids

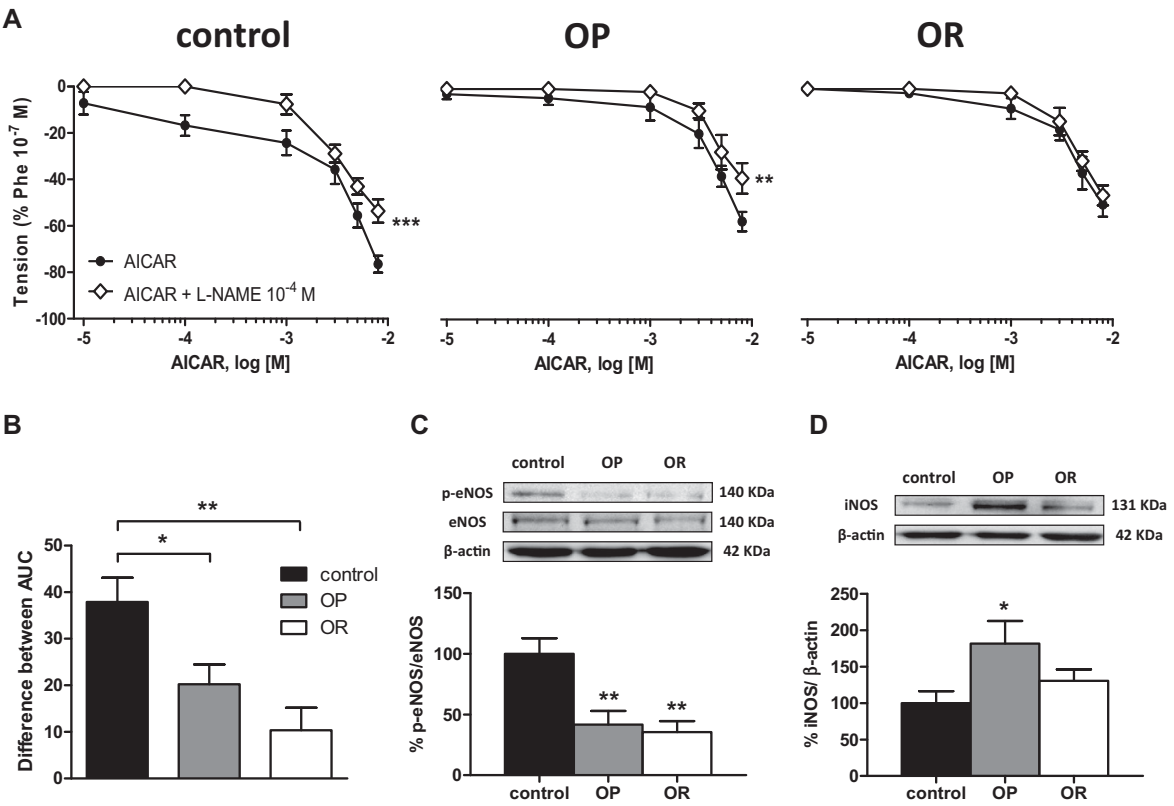

Figure 7. (A) Cumulative concentration-response curves to AICAR (10^{-5} to $8{\cdot}10^{-3}$ M) in presence/absence of L-NAME (10^{-4} M) in +E aorta. $^{**}p < 0.01$ and $^{***}p < 0.001$ compared to their corresponding matched AICAR curves (two-way ANOVA, Bonferroni post hoc test; $n \geq 4$). Data are means ± SEM. (B) Differences between areas under concentration-response curves to AICAR in presence/absence of L-NAME (10^{-4} M) in +E aorta. $^{*}p < 0.05$ and $^{**}p < 0.01$ compared to control group (one-way ANOVA, Newman–Keuls post hoc test; $n \geq 4$). Data are means ± SEM. (C) Representative immunoblots of p-eNOS (Ser^{1177}) in +E aorta and densitometric analysis expressed as percentage of p-eNOS (Ser^{1177})/eNOS in the control group ± SEM. $^{**}p < 0.01$ compared to control animals (one-way ANOVA, Newman–Keuls post hoc test; $n \geq 5$). (D) Representative immunoblots of iNOS in +E aorta and densitometric analysis expressed as percentage of iNOS/β-actin in the control group ± SEM. $^{*}p < 0.05$ compared to control animals (one-way ANOVA, Newman–Keuls post hoc test; $n \geq 5$).

environment but not to BW increase. In fact, the HFD used in this study contains 20% lard, which is rich in palmitate [45]. In addition, the poor management of glucose detected in our HFD rats could also contribute to the alterations observed, as the PI3K/Akt axis is integral to the signaling pathway linked to the insulin receptor in endothelial cells [46]. Moreover, since HFD animals display a poor glucose management, a possible glycosylation of Ser^{1177} residue of eNOS cannot be excluded as a cause of reduced p-eNOS (Ser^{1177}) levels [47].

As suggested by the abolishment of AICAR-induced relaxation in presence of L-NAME in the OR, but not in the OP group, an up-regulation of iNOS was observed in the aorta from this latter group. This is a mechanism probably related to BW increase and not to HFD. Indeed, increased levels of iNOS have been found in different DIO models [48] and showed that HFD in mice increase basal vascular NO bioavailability in part derived from iNOS. In fact, KO mice for iNOS are protected against obesity-induced metabolic insulin resistance despite a similar weight gain of wild type mice [48].

In conclusion, this is the first study demonstrating that HFD leads to endothelial impairment through the down-regulation of the endothelial AMPK–PI3K–Akt–eNOS cascade. This down-regulation is independent of BW gain and is probably related to the rich content of the diet in palmitate and to high blood lipid levels, although a pre-diabetic state could also account for this dysfunction. We propose the endothelial AMPK–PI3K–Akt–eNOS pathway as a possible therapeutic target for the treatment of vascular complications in metabolic disorders related to high energy input. This pathway might be of special relevance since weight loss strategies, such as diet, lifestyle, or behavioral therapy have proven relatively ineffective in improving associated cardiovascular risk factors.

This work was supported by grants from Ministerio de Economía y Competitividad (BFU2012-35353, BFU2011-25303), Grupos UCM (GR-921641), Fundación Universitaria CEU-San Pablo, Fundación Mutua Madrileña, and SESCAMET. CFG-P is recipient of a Ministerio de Educación,

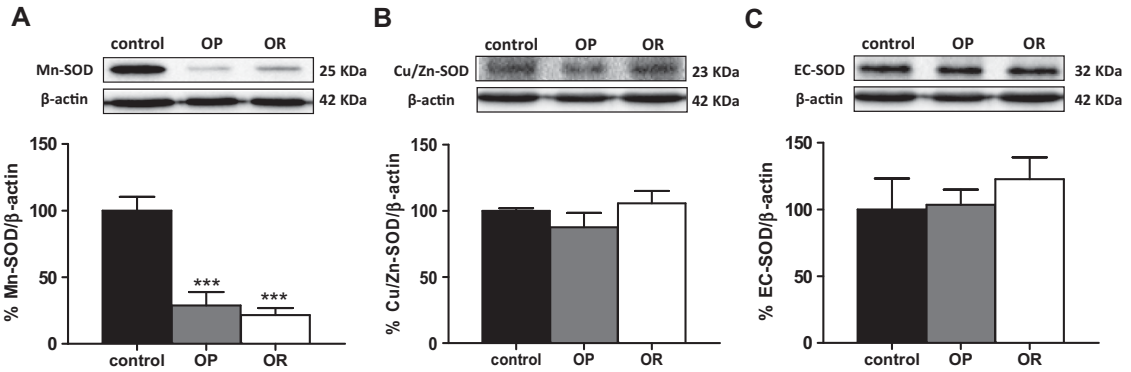

Figure 8. Western blot analysis of superoxide dismutase (SOD) isoforms. (A) Representative immunoblots of Mn-SOD in +E aorta and densitometric analysis expressed as percentage of Mn-SOD/β-actin in the control group ± SEM. $***p < 0.001$ compared to the control group (one-way ANOVA, Newman–Keuls post hoc test; $n = 5$). (B) Representative immunoblots of Cu/Zn-SOD in +E aorta and densitometric analysis expressed as percentage of Cu/Zn-SOD/β-actin in the control group ± SEM ($n = 4$). (C) Representative immunoblots of extracellular SOD (EC-SOD) in +E aorta and densitometric analysis expressed as percentage of EC-SOD/β-actin in the control group ± SEM ($n = 4$).

Cultura y Deporte fellowship. FH-N and DDR are recipients of a CEU-Universidad San Pablo fellowship. GR-H is supported by Juan de la Cierva Program. The funders had no role in study design, data collection and analysis, decision to publish or preparation of the manuscript.

The authors have declared no conflict of interest.

5 References

[1] Hardie D.-G., Carling, D., Carlson, M., The AMP-activated/SNF1 protein kinase subfamily: metabolic sensors of the eukaryotic cell? *Annu. Rev. Biochem.* 1998, *67*, 821–855.

[2] Kahn, B.-B., Alquier, T., Carling, D., Hardie, D.-G., AMP-activated protein kinase: ancient energy gauge provides clues to modern understanding of metabolism. *Cell. Metab.* 2005, *1*, 15–25.

[3] Fisslthaler, B., Fleming, I., Activation and signaling by the AMP-activated protein kinase in endothelial cells. *Circ. Res.* 2009, *105*, 114–127.

[4] Rubin, L.-J., Magliola, L., Feng, X., Jones, A.-W. et al., Metabolic activation of AMP kinase in vascular smooth muscle. *J. Appl. Physiol. (1985).* 2005, *581*, 1163–1171.

[5] Chen, Z.-P., Mitchelhill, K.-I., Michell, B.-J., Stapleton, D. et al., AMP-activated protein kinase phosphorylation of endothelial NO synthase. *FEBS Lett.* 1999, *443*, 285–289.

[6] Chen, Z., Peng, I.-C., Sun, W., Su, M.-I. et al., AMP-activated protein kinase functionally phosphorylates endothelial nitric oxide synthase Ser633. *Circ. Res.* 2009, *104*, 496–505.

[7] Levine, Y.-C., Li, G.-K., Michel, T., Agonist-modulated regulation of AMP-activated protein kinase (AMPK) in endothelial cells: evidence for an AMPK/Rac1/Akt/endothelial nitric-oxide synthase pathway. *J. Biol. Chem.* 2007, *282*, 20351–20364.

[8] Ning, W.-H., Zhao, K., Propionyl-L-carnitine induces eNOS activation and nitric oxide synthesis in endothelial cells via PI3 and Akt kinases. *Vascul. Pharmacol.* 2013, *59*, 76–82.

[9] Morrow, V.-A., Foufelle, F., Connell, J.-M., Petrie, J.-R. et al., Direct activation of AMP-activated protein kinase stimulates nitric-oxide synthesis in human aortic endothelial cells. *J. Biol. Chem.* 2003, *278*, 31629–31639.

[10] Ford, R.-J., Rush, J.-W., Endothelium-dependent vasorelaxation to the AMPK activator AICAR is enhanced in aorta from hypertensive rats and is NO and EDCF dependent. *Am. J. Physiol. Heart. Circ. Physiol.* 2011, *300*, H64–H75.

[11] Lee, K.-Y., Choi, H.-C., Acetylcholine-induced AMP-activated protein kinase activation attenuates vasoconstriction through an LKB1-dependent mechanism in rat aorta. *Vascul. Pharmacol.* 2013, *59*, 96–102.

[12] Bradley, E.-A., Eringa, E.-C., Stehouwer, C.-D.-A., Korstjens, I. et al., Activation of AMP-activated protein kinase by 5-aminoimidazole-4-carboxamide-1-beta-D-ribofuranoside in the muscle microcirculation increases nitric oxide synthesis and microvascular perfusion. *Arterioscler. Thromb. Vasc. Biol.* 2010, *30*, 1137–1142.

[13] Bosselaar, M., Boon, H., van Loon, L.-J.-C., van den Broek, P.-H. et al., Intra-arterial AICA-riboside administration induces NO-dependent vasodilation in vivo in human skeletal muscle. *Endocrinol. Metab.* 2009, *297*, E759–E766.

[14] Horman, S., Morel, N., Vertommen, D., Hussain, N. et al., AMP-activated protein kinase phosphorylates and desensitizes smooth muscle myosin light chain kinase. *J. Biol. Chem.* 2008, *283*, 18505–18512.

[15] Xie, Z., Zhang, J., Wu, J., Viollet, B. et al., Upregulation of mitochondrial uncoupling protein-2 by the AMP-activated protein kinase in endothelial cells attenuates oxidative stress in diabetes. *Diabetes.* 2008, *57*, 3222–3230.

[16] Goirand, F., Solar, M., Athea, Y., Viollet, B. et al., Activation of AMP kinase alpha1 subunit induces aortic vasorelaxation in mice. *J. Physiol.* 2007, *581*, 1163–1171.

[17] Nagata, D., Mogi, M., Walsh, K., AMP-activated protein kinase (AMPK) signaling in endothelial cells is essential for angiogenesis in response to hypoxic stress. *J. Biol. Chem.* 2003, *278*, 31000–31006.

[18] Fisslthaler, B., Fleming, I., Keserü, B., Walsh, K. et al., Fluid shear stress and NO decrease the activity of the hydroxymethylglutaryl coenzyme A reductase in endothelial cells via the AMP-activated protein kinase and FoxO1. *Circ. Res.* 2007, *100*, e12–e21.

[19] Dagher, Z., Ruderman, N., Tornheim, K., Ido, Y., The effect of AMP-activated protein kinase and its activator AICAR on the metabolism of human umbilical vein endothelial cells. *Biochem. Biophys. Res. Commun.* 1999, *265*, 112–115.

[20] Dagher, Z., Ruderman, N., Tornheim, K., Ido, Y., Acute regulation of fatty acid oxidation and amp-activated protein kinase in human umbilical vein endothelial cells. *Circ. Res.* 2001, *88*, 1276–1282.

[21] Blume, C., Benz, P.-M., Walter, U., Ha, J. et al., AMP-activated protein kinase impairs endothelial actin cytoskeleton assembly by phosphorylating vasodilator-stimulated phosphoprotein. *J. Biol. Chem.* 2007, *282*, 4601–4612.

[22] Lee, W.-J., Lee, I.-K., Kim, H.-S., Kim, Y.-M. et al., Alpha-lipoic acid prevents endothelial dysfunction in obese rats via activation of AMP-activate protein kinase. *Arterioscler. Thromb. Vascul. Biol.* 2005, *25*, 2488–2494.

[23] Gálvez, B., de Castro, J., Herold, D., Dubrovska, G. et al., Perivascular adipose tissue and mesenteric vascular function in spontaneously hypertensive rats. *Arterioscler. Thromb. Vasc. Biol.* 2006, *26*, 1297–1302.

[24] Steireif, C., García-Prieto, C.-F., Ruiz-Hurtado, G., Pulido-Olmo, H. et al., Dissecting the genetic predisposition to albuminuria and endothelial dysfunction in a genetic rat model. *J. Hypertens.* 2013, *31*, 2203–2212.

[25] Corton, J.-M., Gillespie, J.-G., Hawley, S.-A., Hardie, D.-G., 5-Aminoimidazole-4-carboxamide ribonucleoside: a specific method for activating AMP-activated protein kinase in intact cells? *Eur. J. Biochem.* 1995, *229*, 558–565.

[26] Somoza, B., Guzmán, R., Cano, V., Merino, B. et al., Induction of cardiac uncoupling protein-2 expression and adenosine 5′-monophosphate-activated protein kinase phosphorylation during early states of diet-induced obesity in mice. *Endocrinology.* 2007, *148*, 924–931.

[27] Bain, J., Plater, L., Elliott, M., Shpiro, N. et al., The selectivity of protein kinase inhibitors: a further update. *Biochem. J.* 2007, *408*, 297–315.

[28] Rutter, G.-A., Da Silva Xavier, G., Leclerc, I., Roles of 5′AMP-activated protein kinase in mammalian glucose homeostasis. *Biochem. J.* 2003, *375*, 1–16.

[29] Trivedi, P., Yang., Barouch L.-A., Decreased p110alpha catalytic activity accompanies increased myocyte apoptosis and cardiac hypertrophy in leptin deficient ob/ob mice. *Cell Cycle.* 2008, *7*, 560–565.

[30] Lelievre, E., Bourbon, P.-M., Duan, L.-J., Nussbaum, R.-L. et al., Deficiency in the p110alpha subunit of PI3K results in diminished Tie2 expression and Tie2(-/-)-like vascular defects in mice. *Blood.* 2005, *105*, 3935–3938.

[31] Thors, B., Halldórsson, H., Thorgeirsson, G., eNOS activation mediated by AMPK after stimulation of endothelial cells with histamine or thrombin is dependent on LKB1. *Biochim. Biophys. Acta.* 2011, *1813*, 322–331.

[32] Colombo, S.-L., Moncada, S., AMPKalpha1 regulates the antioxidant status of vascular endothelial cells. *Biochem. J.* 2009, *421*, 163–169.

[33] Ko, H.-J., Zhang, Z., Jung, D.-Y., Jun, J.-Y. et al., Nutrient stress activates inflammation and reduces glucose metabolism by suppressing AMP-activated proteinkinase in the heart. *Diabetes.* 2009, *58*, 2536–2546.

[34] Muse, E.-D., Obici, S., Bhanot, S., Monia, B.-P. et al., Role of resistin in diet-induced hepatic insulin resistance. *J. Clin. Invest.* 2004, *114*, 232–239.

[35] Wu, Y., Song, P., Xu, J., Zhang, M. et al., Activation of protein phosphatase 2A by palmitate inhibits AMP-activated protein kinase. *J. Biol. Chem.* 2007, *282*, 9777–9788.

[36] Bakker, S.-J., Ijzerman, R.-G., Teerlink, T., Westerhoff, H.-V. et al., Cytosolic triglycerides and oxidative stress in central obesity: the missing link between excessive atherosclerosis, endothelial dysfunction, and beta-cell failure? *Atherosclerosis.* 2000, *148*, 17–21.

[37] Madamanchi, N.-R., Moon, S.-K., Hakim, Z.-S., Clark, S. et al., Differential activation of mitogenic signalling pathways in aortic smooth muscle cells deficient in superoxide dismutase isoforms. *Ateriosclerosis. Thromb. Vasc. Biol.* 2005, *25*, 950–956.

[38] Fridovich, I., Fundamental aspects of reactive oxygen species, or what's the matter with oxygen? *Ann. N. Y. Acad. Sci.* 1999, *893*, 13–18.

[39] Williams, M.-D., Van Remmen, H., Conrad, C.-C., Huang, T.-T. et al., Increased oxidative damage is correlated to altered mitochondrial function in heterozygous manganese superoxide dismutase knockout mice. *J. Biol. Chem.* 1998, *273*, 28510–28515.

[40] Levin, B.-E., Triscari, J., Sullivan, A.-C., Relationship between sympathetic activity and diet-induced obesity in two rat strains. *Am. J. Physiol.* 1983, *245*, R364-R371.

[41] Dobrian, A.-D., Davies, M.-J., Prewitt, R.-L., Lauterio, T.-J., Development of hypertension in a rat model of diet-induced obesity. *Hypertension.* 2000, *35*, 1009–1015.

[42] Dobrian, A.-D., Davies, M.-J., Schriver, S.-D., Lauterio, T.-J. et al. Oxidative stress in a rat model of obesity-induced hypertension. *Hypertension.* 2001, *37*, 554–560.

[43] Boustany, C.-M., Bharadwaj, K., Daugherty, A., Brown, D.-R. et al., Activation of the systemic and adipose renin-angiotensin system in rats with diet-induced obesity and hypertension. *Am. J. Physiol. Regul. Integr. Comp. Physiol.* 2004, *287*, R943–R949.

[44] Boustany, C.-M., Brown, D.-R., Randall, D.-C., Cassis, L.-A., AT1-receptor antagonism reverses the blood pressure elevation associated with diet-induced obesity. *Am. J. Physio.l Regul. Integr. Comp. Physiol.* 2005, *289*, R181–R186.

[45] Rohman, A., Triyana, K., Sismindari, Erwanto, Y., Differentiation of lard and other animal fats based on triacylglycerols composition and principal component analysis. *Int. Food Res. J.* 2012, *19*, 475–479.

[46] Zeng, G., Nystrom, F.-H., Ravichandran, L.-V., Cong, L.-N. et al., Roles for insulin receptor, PI3-kinase, and Akt in

insulin-signaling pathways related to production of nitric oxide in human vascular endothelial cells. *Circulation.* 2000, *101*, 1539–1545.

[47] Musicki, B., Kramer, M.-F., Becker, R.-E., Burnett, A.-L., Inactivation of phosphorylated endothelial nitric oxide synthase (Ser-1177) by O-GlcNAc in diabetes-associated erectile dysfunction. *Proc. Natl. Acad. Sci. USA.* 2005, *102*, 11870–11875.

[48] Noronha, B.-T., Li, J.-M., Wheatcroft, S.-B., Shah, A.-M. et al., Inducible nitric oxide synthase has divergent effects on vascular and metabolic function in obesity. *Diabetes.* 2005, *54*, 1082–1089.

